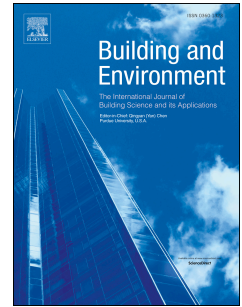# Accepted Manuscript

Indoor and outdoor particles in an air-conditioned building during and after the 2013 haze in Singapore

Ailu Chen, Qingliang Cao, Jin Zhou, Bin Yang, Victor W.-C. Chang, William W. Nazaroff

Please cite this article as: Chen A, Cao Q, Zhou J, Yang B, Chang VW-C, Nazaroff WW, Indoor and outdoor particles in an air-conditioned building during and after the 2013 haze in Singapore, *Building and Environment* (2016), doi: 10.1016/j.buildenv.2016.01.002.

20 June 2013 (9 AM)   8 July 2013 (9 AM)

Indoor and outdoor particles in an air-conditioned building during and after the 2013 haze in Singapore

Ailu Chen[1, 2], Qingliang Cao[1], Jin Zhou[1, 2], Bin Yang[3], Victor W.-C. Chang[1, 2*], William W Nazaroff[2, 4]

[1]School of Civil and Environmental Engineering, Nanyang Technological University, 50 Nanyang Avenue 639798, Singapore

[2]SinBerBEST Program, Berkeley Education Alliance for Research in Singapore (BEARS), 1 CREATE Way, University Town 138602, Singapore

[3]Department of Applied Physics and Electronics, Umeå University, Umeå 90187, Sweden

[4]Department of Civil and Environmental Engineering, University of California, 760 Davis Hall, Berkeley, California 94720, United States

[*]Corresponding Author: Tel: +65-6790-4773, Fax: +65-6792-1650, E-mail: *wcchang@ntu.edu.sg*

Abstract

Particles released from biomass burning can contribute to severe air pollution. We monitored indoor and outdoor particles in a mechanically ventilated and air-conditioned building during and after the 2013 haze event in Singapore. Continuous monitoring of time-and size-resolved particles in the diameter range 0.01-10 µm was conducted for two weeks in each sampling campaign. During the haze event, the averaged size-resolved outdoor particle volume concentrations ($dV/d(\log D_p)$) for diameters larger than 0.3 µm were considerably higher than those during the post-haze days (9-185 µm^3 cm^{-3} versus 1-35 µm^3 cm^{-3}). However, the average number concentration of particles with diameters in the range 10-200 nm was substantially lower on the hazy days than on the post-haze days (11,400 to 14,300 particles cm^{-3} for hazy days, versus an average of 23,700 particles cm^{-3} on post-haze days). The building mechanical ventilation system, equipped with MERV 7 filters, attenuated the penetration and persistence of outdoor particles into the monitored building. Indoor particle concentrations, in the diameter ranges 0.3-1.0 µm and 1.0-2.5 µm, closely tracked the

28 corresponding patterns of outdoor particle concentrations. For particles in the size range

29 0.01-1.0 µm, the size-resolved mean indoor/outdoor (I/O) ratios were in the range 0.12-0.65

30 with the highest mean I/O ratio at 0.3 µm (0.59 in AC on mode and 0.64 in AC off mode).

31 The air conditioning and mechanical ventilation system with MERV 7 filters provided low

32 single-pass removal efficiency (less than ~ 30%) for particles with diameters of 0.01-1.0 µm.

33 During the haze, for particles larger than ~ 0.2 µm, lower I/O ratios and higher removal

34 efficiencies occurred with the air conditioning operating as compared to with mechanical

35 ventilation only. This observation suggests the possibility of particle loss to air conditioning

36 system surfaces, possibly enhanced by thermophoretic or diffusiophoretic effects.

37 **Keywords**: Indoor-outdoor relationship, Aerosol, Landscape fires, Pollutants, Particulate

38 matter

39 **1. Introduction**

40 Two types of large, uncontrolled combustion can contribute to regional-scale air pollution

41 episodes. Wildfires are common seasonal occurrences especially in semiarid regions such as

42 the western United States and Australia. The use of large-scale biomass burning to clear land

43 for agriculture is an important environmental issue in Southeast Asia. Such burning causes

44 air quality problems because of the heavy emissions of combustion byproducts followed by

45 atmospheric transport and dispersion plus photochemical transformation processes that create

46 regional pollution episodes. Prior studies have investigated certain characteristics of airborne

47 particulate matter associated with uncontrolled biomass burning, such as the organic and

48 elemental carbon (OC/EC) composition of air [1, 2], biomass burning signatures of individual

49   particles [3], trace elements in particulate matter [4, 5] and particle-bound polycyclic

50   aromatic hydrocarbons (PAHs) [5, 6].

51   Particles originating from biomass burning might have significant impacts on human health.

52   For example, such particles are demonstrated to be more toxic to lung macrophages than

53   other ambient particles [7]. Particles from wildfires can induce pro-inflammatory responses

54   [8] and contribute to oxidative stress [9]. A large wildfire in southern California was found

55   to result in a "significant increase in hospital emergency room visits for asthma, respiratory

56   problems, eye irritation, and smoke inhalation" [10]. Because of their potential contributions

57   to the degradation of public health, it is worthwhile to pursue a deeper understanding of

58   airborne particulate matter associated with uncontrolled biomass burning episodes.

59   Particle size is a key parameter, not only influencing dynamic behavior but also for assessing

60   human health risks [11]. A few studies have documented that biomass burning activities can

61   alter the airborne particle size distribution in the impacted area [12, 13]. Increases in particle

62   mass concentrations are observed in the accumulation mode (0.1-2.0 µm). Particles in this

63   size range contribute strongly to visibility impairment, a commonly observed adverse impact

64   of large-scale biomass burning. Increases are also reported for the coarse mode (> 2.0 µm).

65   However, decreases have been observed in the nucleation mode (diameter smaller than 0.1

66   µm). These findings highlight the importance of dynamic processes that influence the

67   evolution of the particle size distribution. For example, growth induced by the condensation

68   of semivolatile vapors would tend to shift nucleation mode particles toward the accumulation

69   mode. It is important to better understand the size distributions of airborne particles

70   associated with biomass burning events.

71   The penetration and persistence of particles from outdoor to indoor air is important with

72   regard to health because people spend a large fraction of their time indoors [14]. When

73   outdoor pollution levels are high, as during biomass burning episodes, people may be advised

74   to curtail activities and remain indoors as a "shelter-in-place" strategy. For an office

75   building, the major pathway connecting the indoor environment to outdoor air is the heating,

76   ventilating and air-conditioning (HVAC) system [15]. For tropical climates such as in

77   Singapore, heating is seldom or never needed, and so the analogous term, which we shall use

78   in this paper, is the air-conditioning and mechanical ventilation (ACMV) system.

79   Several studies have reported that submicron particle number concentrations in office

80   buildings closely follow the corresponding outdoor concentrations in the absence of a strong

81   indoor source [16, 17, 18]. Among the factors that can affect the particle indoor/outdoor

82   ratios (I/O) are particle size [19], air-exchange rate (AER) [19], and filter efficiency [16].

83   Indoor concentrations of particles originating outdoors can be reduced by improving filter

84   efficiency [20]. Shi et al. [21] have reported laboratory tests that document the size-

85   dependent particle removal efficiency of filters commonly used in ventilation systems.

86   However, indoor-outdoor relationships have not been extensively reported for office

87   buildings in relation to air pollution episodes caused by uncontrolled biomass burning. It is

88   worthwhile to better understand the performance of normally used filters in office buildings

89   for removing particles of outdoor origin, especially when the outdoor levels are episodically

90   elevated, as during the 2013 haze in Singapore.

91   During the Southeast Asia haze episode of June 2013, the outdoor $PM_{2.5}$ concentrations rose

92   to 250 μg m^{-3} on the most polluted days. This order-of-magnitude elevation above the

93   normal ambient $PM_{2.5}$ concentration of 15-25 μg m^{-3} provided an opportunity to investigate

94   the relationship between indoor and outdoor particle levels in a mechanically ventilated and

95   air-conditioned building when the outdoor particle level was unusually high. The current

96   study presents monitoring results and their interpretation considering size- and time-resolved

97   indoor and outdoor particle concentrations both during the 2013 haze and on low-pollution

98   days after the haze episode. The study aims to provide information and contribute new

99   knowledge regarding four important features at the intersection of regional air pollution

100   episodes, building environmental systems, and human exposure: 1) size-resolved outdoor

101   particle volume and number concentrations measured in Singapore with and without episodic

102   haze; 2) size-resolved indoor and outdoor particle relationships in a typical office building; 3)

103   influence of ACMV operation modes on these relationships (i.e., with and without operating

104   the air-conditioning cooling coil); and 4) performance of a typical ACMV system on

105   reducing the penetration and persistence of outdoor particles indoors.

106 **2. Material and Methods**

107 *2.1. Monitoring sites*

108 Outdoor and indoor monitoring was undertaken on the campus of Nanyang Technological

109 University (NTU). The NTU campus, located in western Singapore, is bordered by forested

110 land to the north and west, by industrial areas to the south, and by residential areas to the east.

111 On hazy days, the adjacent areas are not likely to have contributed substantially to the

112 outdoor particle concentrations, as evidenced by the small variation in $PM_{2.5}$ concentrations

113 across the five government-operated monitoring stations that span the city [22]. The

114 sampling sites were on the western side of the campus, situated about 200 m from the forest.

115 Vehicular traffic on the campus is small, consisting mainly of light-duty passenger cars for

116 commuters. There are no other noteworthy particle sources on campus.

117 The present study reports results from two monitoring campaigns, with conditions that we

118 will refer to as "hazy" and "clear sky," respectively. The hazy campaign spanned 14-29 June

119 2013 and the clear sky campaign took place 13-26 August 2013. Monitoring sites were the

120 same for both campaigns. The outdoor monitoring station was sited on the balcony of a

121 lecture theatre, with the air inlet positioned 12 m above the ground. The indoor station was

122 20 m away from the outdoor monitoring station and about 1.2 m above the floor. The fresh

123 air intake of the ACMV system was situated at a height of 21 m above the ground and at 20

124 m horizontal distance from the outdoor monitoring station. Given the strong regional impact

125 of the air pollution episode and the small contribution of local sources, we believe that the

126 outdoor monitoring results reflect accurately the conditions prevailing in the ventilation air

127   supplied to the indoor site. The room where the indoor station was placed had a hard-surface

128   floor of area 19 m^2 and was part of a staff office. The office had an area of 300 m^2 and had

129   been unoccupied for more than one year. Polyvinyl chloride flooring covered five-sixths of

130   the office's floor surfaces and the remaining floor area was carpeted. The office also

131   contained basic furniture such as tables, cabinets, and chairs. There were no obvious indoor

132   particle sources. The room had casement windows and curtains; windows and doors were

133   closed throughout both monitoring campaigns.

134   The air-handling unit (AHU) that served the office had an independent ventilation system

135   (Figure 1), so the office was isolated from other rooms in the same building. When the

136   mechanical ventilation was operating, make-up air accounted for ~ 10% of the volume flow

137   rate of supply air. The make-up air mixed with the recirculated air first and then the air

138   mixture passed through the filter and coil as shown in Figure 1. When the MV system was

139   on, the office was slightly pressurized by the supplied air; such pressurization would have

140   prevented outdoor air from substantially infiltrating into the office, making flow through the

141   ACMV system the dominant pathway of fresh air supply and outdoor particle penetration.

142   The filters in the AHU had a grade of MERV 7, which means its nominal removal efficiency

143   is 25-35% for particles with diameters of 0.3-10.0 μm. In addition, its minimum removal

144   efficiencies for particles with diameters of 0.3-1.0 μm, 1.0-3.0 μm and 3.0-10.0 μm are 17%,

145   46% and 50%, respectively [23].

146   When air conditioning was employed, chilled water circulating through the coil had a

147   temperature of 7 °C. In normal practice at NTU, filters are replaced and cooling coils are

148   cleaned concurrently at intervals of three months. From June to August 2013, the filters were

149   not replaced and the cooling coils were not cleaned. When the mechanical ventilation was on,

150   the air exchange rate of the office was 3.8 h^{-1}, whereas when the system was off, the average

151   air exchange rate (owing to leakage) was 0.5 h^{-1}.

152   The ACMV system was operated in three different modes during the two monitoring

153   campaigns. During weekdays of both the hazy and the clear-sky periods, the ACMV system

154   was on (Mode 1: air conditioning and mechanical ventilation on) from 7:30 to 18:30.

155   Overnight during the haze period, i.e. 18:30 to 7:30 on the next day, the AC was off but the

156   MV system continued to operate (Mode 2: air conditioning off, mechanical ventilation on).

157   During the weekday overnight intervals of the clear-sky period, the ACMV system was off

158   (Mode 3: air conditioning and mechanical ventilation off). For weekends (both daytime and

159   overnight), Mode 2 was applied during the haze period and Mode 3 was applied for the clear-

160   sky days.

161   *2.2. Instruments*

162   During both campaigns, size- and time-resolved concentrations of both indoor and outdoor

163   particles with diameters in the range 0.01 μm to 10 μm were concurrently monitored for

164   multiple days. Particles with diameters of 0.01 μm to 0.2 μm were measured with TSI

165   Nanoscan SMPS Nanoparticle Sizers (Model 3910, TSI Inc., Shoreview, USA). The SMPS

8

166   uses isopropyl alcohol (purity $\geq$ 99.7%, Sigma-Aldrich) as the reagent and can measure

167   particle number concentrations in the range 100-1,000,000 cm^{-3}. For larger particles, 0.3-10

168   µm in diameter, TSI optical particle sizers (OPS, Model 3330) were employed. These can

169   measure particle concentrations up to 3,000 cm^{-3} and optically resolve particles into 16 size

170   channels. Temperature and relative humidity were measured using TSI VelociCalc Air

171   Velocity meters (model 9545-A). Monitoring was conducted continuously every day and

172   measurement results were recorded at intervals of 1 min. However, with high water vapor

173   content in Singapore's air, we found that the SMPSs only functioned properly (i.e. without

174   reporting error) during some portions of each day. Consequently, we have relatively small

175   datasets from the SMPSs in the current study.

176   An InfraRan Specific Vapor Analyzer (Wilkes Enterprise Inc., East Norwalk, USA) was used

177   to measure the air exchange rates of the indoor environment based on the tracer gas decay

178   method, using sulfur hexafluoride as the tracer.

179   *2.3. Outdoor weather conditions*

180   In accordance with expectations for Singapore's tropical climate, the outdoor weather

181   conditions were similar during each sampling campaign. Table S1 presents a summary of

182   selected outdoor atmospheric parameters and $PM_{2.5}$ mass concentrations for the two

183   campaigns. The $PM_{2.5}$ mass concentration presented in Table S1 of each day was calculated

184   based on outdoor sized-resolved particle number concentrations monitored by outdoor OPS

185   and SMPS with assumed particle density of 1.0 g cm^{-3} [22]. During the hazy period,

9

186   temperatures were between 25 and 35 °C and the relative humidity was 40-90%. The

187   average daily wind speed was mainly in the range 5-8 km h^{-1} (except for 19-20 June) and

188   from the southwest. Though it was during the monsoon season, there were only four

189   precipitation events (June 16, 24, 25 and 26). During the clear-sky campaign, air

190   temperatures were mainly between 27 and 32 °C and relative humidity was mainly between

191   50 and 90%. Mean wind speeds were mainly 4-8 km h^{-1} and were primarily from the south.

192   There were six precipitation episodes during the clear-sky monitoring campaign. Given the

193   similar weather conditions, the influence of meteorological conditions on outdoor particles is

194   expected to be comparable for the two campaigns.

195   *2.4. Data analysis and quality assurance*

196   A clear difference is seen between the overall outdoor $PM_{2.5}$ concentrations of these two

197   campaigns (Table S1). According to data reported by Singapore's National Environmental

198   Agency (NEA), during the 2013 haze episode, the daily averaged outdoor $PM_{2.5}$

199   concentrations ranged from 38 to 268 µg m^{-3} and the average $PM_{2.5}$ concentration was 96 µg

200   m^{-3}. Utilizing NEA data, and based on the daily-average outdoor $PM_{2.5}$ concentrations, we

201   classified the hazy days into three categories: heavy haze ($PM_{2.5} > 150$ µg m^{-3}), moderate

202   haze (60-150 µg m^{-3}) and light haze (35-60 µg m^{-3}). During the clear-sky periods, the daily

203   averaged outdoor $PM_{2.5}$ concentrations normally ranged from 10 to 30 µg m^{-3} and the average

204   $PM_{2.5}$ concentration was approximately 20 µg m^{-3}.

205   Measured particle, temperature and RH results were first processed to exclude errors owing

206   to instrument malfunction. Indoor and outdoor data were then paired as linked time series.

207   For particles in the diameter range 0.01-10 μm, count concentrations were converted to

208   volume concentrations based on the method reported in Zhou et al [22]. All data were

209   arranged day-by-day and days that had complete data without evidence of error (i.e. owing to

210   instrument malfunction) were chosen to compute outdoor size-resolved particle volume

211   concentrations ($dV/dlog\,D_p$) and number concentrations ($dN/dlog\,D_p$). Size-resolved outdoor

212   particle data for 19-22 June were averaged to represent the heavy haze days; data for 16-18

213   and 23 June were averaged to represent moderate haze conditions, data on 24-25 and 27-29

214   June were used to represent light-haze days, and measurements from 16-17 and 21-23 August

215   were applied to represent the clear-sky conditions. In all, seventeen days were selected for

216   further analysis, considering data availability as the major criterion. Days that had

217   continuously valid data for less than three hours were excluded to limit errors in determining

218   I/O ratios owing to lag time. In preliminary data processing, we only accepted data for which

219   there was no error reported by either particle-monitoring instrument or otherwise recorded in

220   our logbook.

221   Data records for the time period 10:00 to 18:00 on days with valid data were chosen for

222   calculating I/O ratios for Mode 1. Data records from 20:00 to 6:00 of their next day were

223   chosen for analysis for Mode 2 conditions. Data recorded close to the transition periods of

224   the ACMV system (i.e., 6:00-10:00 each weekday morning and 18:00-20:00 each weekday

225   evening) were excluded to avoid potential biases caused by time-varying indoor

226   temperatures. One-way ANOVA tests were performed to compare size-resolved I/O ratios

227   under different ACMV operation modes. We applied a probability of 0.05 as the threshold in

228   testing for statistical significance (SPSS 22, IBM Inc., USA).

229   We conducted side-by-side tests for both the SMPSs and OPSs during light-haze and clear-

230   sky periods with outdoor $PM_{2.5}$ concentrations between 20 $\mu g\ m^{-3}$ and 60 $\mu g\ m^{-3}$. Adjustment

231   factors based on these comparisons were applied to minimize the differences between

232   individual instruments throughout the whole monitoring period. The side-by-side tests were

233   carried out in the room where the indoor station was placed. The test duration for the SMPSs

234   was 22.5 h and that for the OPSs was 21 h. In the tests, the monitors recorded data at 1-min

235   intervals, which was consistent with the indoor and outdoor monitoring experiments. We

236   calculated the adjustment factor for each channel using the average of readings in that

237   channel from the paired monitors as a reference value. In each channel, the reference values

238   were averaged over the whole test period and the average was divided by average of readings

239   from each monitor. The calculated adjustment factors are listed in Table S2. The paired

240   monitors were reasonably consistent with each other for both SMPSs and OPSs with most

241   differences smaller than 15%.

242   *2.5. Estimates of particle removal efficiencies of the ACMV system*

243   We estimated size-resolved single-pass particle removal efficiencies of the ACMV system,

244   which are believed to be mainly attributable to the MERV 7 filters. Various ACMV

245   components, including filters, coils, and ducting, may contribute to particle removal when the

12

246 system was operating; however, filters are believed to contribute the most to removal as other

247 components should play limited roles, especially for fine particles [24, 25]. The filters

248 remove the majority of coarse particles as they are the first layer of defense in the ACMV

249 system (as shown in Figure 1) and they have much higher removal efficiency for coarse

250 particles than for fine and ultrafine particles.

251 Equation 1, based on material balance, describes the time dependent indoor particle number

252 concentration:

$$\frac{dN_{i,in}}{dt} = \lambda N_{i,out}(1-\eta_i) - \lambda_r N_{i,in}\eta_i - \beta_i N_{i,in} - \lambda N_{i,in} \tag{1}$$

253 Here, $N_{i,in}$ is the indoor number concentration of particles in the ith size bin (particles cm^{-3}); t

254 is time (h); $N_{i,out}$ is the outdoor number concentration of particles in the ith size bin (particles

255 cm^{-3}); λ is the air-exchange rate (h^{-1}); η_i is single-pass removal efficiency of the ACMV

256 system for particles in size bin i (unitless); λ_r is the recirculation rate of the indoor air in the

257 ACMV system (h^{-1}); and β_i is the indoor deposition rate of particles in the ith size bin (h^{-1}). In

258 developing Equation 1, we assumed balanced volumetric flows (appropriate for near-

259 isothermal conditions), no particle resuspension or generation indoors, no coagulation of

260 particles, and no phase-change processes. We also assumed that during monitoring, when the

261 mechanical ventilation was on, there was no particle infiltration from outdoors to indoors that

262 would bypass the filter. In addition, we assumed that the air-exchange rate of the indoor

263 environment was constant. We treated the filter efficiencies for particles of specific sizes to

264   be identical for makeup and recirculated air, since there are no separate prefilters in the

265   system.

266   To solve Equation 1, we apply time averaging, neglecting any change of particle number

267   concentration in the indoor environment and assuming that $N_{i,in}$ and $N_{i,out}$ are not correlated in

268   time with λ, η_i, λ_r or β_i. The result is Equation 2:

$$\frac{\overline{N_{i,in}}}{\overline{N_{i,out}}} = \frac{\lambda(1-\eta_i)}{\lambda_r\eta_i + \beta_i + \lambda} \tag{2}$$

269   Here, $\overline{N_{i,in}}$ is the indoor time-averaged number concentration of particles in the ith size bin

270   (particles cm^{-3}) and $\overline{N_{i,out}}$ is the corresponding outdoor value (particles cm^{-3}). Considering

271    $\overline{N_{i,in}} / \overline{N_{i,out}} = (I/O)_i$, we transformed Equation 2 to Equation 3 for calculating removal

272   efficiency of the ACMV system for particles in each size bin:

$$\eta_i = \frac{\lambda - (\beta_i + \lambda)(I/O)_i}{\lambda + \lambda_r(I/O)_i} \tag{3}$$

273   Here, $(I/O)_i$ is time-averaged ratio of indoor to outdoor particle concentrations in the ith size

274   bin (unitless). Before undertaking the calculations, we first estimated the size-resolved

275   indoor particle deposition rates (β_i). In this study, the β_i values are based on the deposition

276   model developed by Riley et al. [26]. Table S3 presents the calculated β_i value for each

277   effective particle size. In the indoor environment, as shown in Figure 1, the air exchange rate

278   was 3.8 h^{-1} and the recirculation rate was 34.2 h^{-1}. Size-resolved particle removal efficiencies

279   of the ACMV system when it was operated in both Mode 1 (both AC on and MV on) and

280   Mode 2 (AC off and MV on) were computed based on the corresponding measured particle

281   I/O ratios, utilizing Equation 3.

3.   Results and Discussion

3.1. Summary of indoor and outdoor particle number concentrations

284   Table S4 summarizes the time-weighted and size-resolved indoor and outdoor particle

285   number concentrations during and after the 2013 haze. For all haze levels, particles smaller

286   than 0.37 μm account for most particles by number. In each size range, the indoor

287   concentrations were always lower than the corresponding outdoor concentrations.

3.2. Size-resolved outdoor particle concentrations

289   Figure 2 illustrates time-averaged volume-weighted size distributions (dV/dlog D_p) measured

290   outdoors for particles with diameters 0.01-10 μm for the four haze conditions. Overall,

291   particle volume concentrations for the heavy haze days are approximately seven times higher

292   than on clear-sky days, with ratios ranging from 4 to 60 across particle sizes. Compared with

293   the clear-sky days, the total volume concentration is two times higher for light haze and five

294   times higher for moderate haze. It is noteworthy that submicron particles account for

295   approximately half (45-54%) of the total volume distribution for hazy days, whereas the

296   percentage was smaller (35%) for clear-sky conditions. There is an evident shift in the peak

297   of the submicron size distribution as the haze level increases. The peak diameter was 0.18

298   μm for clear-sky conditions and progressively increased to approximately 0.42 μm for the

299   moderate and heavy haze days. This observation suggests the occurrence of substantial

15

300   secondary growth of particles probably owing to a combination of condensation and

301   coagulation during the haze episode.

302   Figure 3 illustrates the time-averaged and size-resolved particle number distribution (dN/dlog

303   D_p) for particles with diameters of 0.01-10 μm, again sorted according to haze level. The

304   striking feature of this figure is the prominence of a count-weighted peak, centered at a

305   diameter of about 0.07 μm diameter, for clear-sky conditions. For hazy conditions, the peak

306   shifts to a larger particle size of about 0.2 μm diameter, for which light scattering would be

307   much more efficient.

308   Total number concentrations of ultrafine particles (0.01-0.2 μm) for hazy days were less than

309   measured for clear-sky conditions. Specifically, levels were $13,100 \pm 6,500$, $11,400 \pm 4,800$,

310   and $14,300 \pm 10,800$ particles cm^{-3} for heavy, moderate and light haze days, respectively,

311   versus $23,700 \pm 9,200$ particles cm^{-3} for clear-sky conditions. Qualitatively similar

312   observations have been reported by Betha et al. [27] and Mielonen et al. [28].

313   A plausible factor contributing to the shift in sizes is the different sources of ultrafine

314   particles and the associated growth processes. On hazy days, the primary source of

315   submicron particles over Singapore would be the agricultural fires in Sumatra, approximately

316   300 km to the west (as shown in Figure S1). It would take a day or two for pollutants emitted

317   from this locale to travel to Singapore. The time scale would enable the ultrafine particles to

318   grow to sizes larger than 0.10 μm in diameter [29]. Figure 3 shows that the count-weighted

319   size distribution has a peak at approximately 0.17 μm for both the heavy and moderate haze

320   days, whereas the peak occurs at 0.07 μm on the clear-sky days. For clear-sky conditions,

321   probable sources of ultrafine particles measured in Singapore would be local emissions,

322   including industrial and vehicular activities [30]. The proximity of these sources to the

323   monitoring station offers much less time for ultrafine particle to grow through

324   photochemically driven condensation.

325   Additional evidence about the importance of time for condensational growth of haze particles

326   can be found in comparing the 2013 haze episode here to a 2009 haze event triggered by local

327   biomass burning in Singapore [30]. During the 2009 haze, the mean hourly total particle

328   number concentration was 37,800 particles cm^{-3} (5.6-560 nm), which was 3× that in the

329   current study. During the 2009 haze, there was little time for newly generated ultrafine

330   particles to grow to submicron particles given the close proximity between the monitoring

331   and emissions sites. Differences in the peak diameters of the count-weighted size distribution

332   (0.17 μm during the 2013 haze *versus* 0.06 μm during the 2009 episode) highlight the

333   importance of reaction time as a factor influencing particle size distributions.

334   The findings shown in Figures 2 and 3 indicate that particles larger than 0.1 μm contributed

335   the most to the outdoor particle pollution during the 2013 haze episode. The findings

336   improve our understanding of the size distributions of particles originating from agricultural

337   biomass burning upwind of Singapore. Because of the frequent recurrence of transboundary

338   haze in Singapore, knowledge about particle size-distributions is useful for developing

339   technology and policy to mitigate the adverse effects of haze particles. In Section 3.3, we

340   evaluate indoor-outdoor relationships for particles in a mechanically ventilated building.

341   Since the ultrafine particle concentrations were observed not to increase during the haze, we

342   focus on particles with diameters of 0.3-10 μm and consider whether there are systematic

343   differences among the four different outdoor pollution conditions.

344   *3.3. Time-resolved outdoor and indoor particle concentrations*

345   Figure 4 shows time-resolved indoor and outdoor particle volume concentrations (μm^3 cm^{-3})

346   in three size bins (0.3-1.0 μm, 1.0-2.5 μm and 5.0-10.0 μm) for one typical day each for the

347   heavy, moderate, and light haze conditions. In Figure 4, the ACMV was operating in Mode 1

348   (AC on + MV on) for 07:30-18:30 and in Mode 2 (AC off + MV on) for other times.

349   Figure 4 frames a, b, and c show that indoor particle concentrations in the size range 0.3-1.0

350   μm were always lower than the corresponding outdoor concentrations. Furthermore,

351   concentrations of these smaller sized particles tracked the corresponding outdoor

352   concentrations closely throughout the day. Temporal patterns of indoor concentrations were

353   attenuated and delayed when compared with the corresponding outdoor concentrations. The

354   indoor concentration was approximately half of the outdoor concentration. This attenuation

355   is mainly attributable to the ACMV system's filtration effects on outdoor particles in the

356   process of transporting air from outdoors to indoors and recirculating it; otherwise, the indoor

357   environment is well isolated from the outdoors by the building envelope. The data also

358   reveal a time lag of approximately 15 min between sudden changes in outdoor concentrations

359   and corresponding changes indoors. That lag is consistent expectations: it is approximately

18

360   the reciprocal of the measured air-exchange rate of 3.8 h^{-1}. For the three haze conditions,

361   indoor average volume concentrations for particles sized 0.3-1.0 µm were 43.6 µm^3 cm^{-3},

362   20.5 µm^3 cm^{-3}, and 5.5 µm^3 cm^{-3}, respectively; each of these values is higher than that for the

363   clear-sky conditions (4.8 µm^3 cm^{-3}).

364   For particles with diameters in the range 1.0-2.5 µm, indoor concentrations were much lower

365   than corresponding outdoor concentrations (Figure 4 frames d, e, and f). Impaction and

366   interception control particle filtration efficiency in this size range and are much more

367   efficient for these particles than for those in the 0.3-1 µm diameter range, for which the

368   ACMV system exhibited a weaker attenuation effect [31]. For the 1.0-2.5 µm diameter range,

369   indoor peak concentrations are approximately 20% of the corresponding outdoor peak

370   concentrations. Despite attenuation, indoor concentrations were still notably higher when the

371   outdoor concentrations were elevated during the haze. For heavy, moderate and light haze

372   days, the indoor mean volume concentrations in this size bin were 8.1, 7.6 and 1.1 times the

373   clear-sky values, respectively.

374   For particles in the diameter range 2.5-10.0 µm, there is no evident temporal covariation

375   between indoor and outdoor concentrations (Figure 4 frames g, h, and i). The indoor volume

376   concentrations of particles in the diameter range 2.5-10.0 µm were consistently lower than 5

377   µm^3 cm^{-3} and were comparable across the different haze intensities, even though the outdoor

378   concentrations were markedly different for these days. These findings indicate that the

379   ACMV system in this building effectively protects occupants against outdoor particles larger

380   than 2.5 µm. The effectiveness of the ACMV system in limiting penetration and persistence

381   of these coarse particles from outdoors results from the high proportion of recirculation flow

382   (90%). Even though the single-pass efficiency of the MERV 7 filters is only moderate, the

383   multiple passes of indoor air through the filters yields a high overall effectiveness in reducing

384   airborne coarse particle concentrations.

385   In Section 3.2, we reported that particles larger than 0.1 µm dominated the particle volume or

386   mass concentrations during the haze. Here, we have shown that the ACMV system was

387   effective at removing particles larger than 2.5 µm under normal operation. Combining this

388   information, we could state that, in the absence of important indoor particle sources,

389   occupants of a building with a conventional ACMV system during the haze episode would

390   mainly be exposed to particles in the diameter range 0.1-2.5 µm. Recognizing the importance

391   of adverse human health effects associated with exposure to fine particles, it would be of

392   scientific and public health value to develop improved strategies to mitigate indoor fine

393   particle pollution from outdoor sources in this size range, especially during occasions of

394   extreme outdoor pollution such as the Singapore 2013 haze. Such information might assist

395   government agencies in setting policies to protect building occupants from excessive particle

396   exposure during haze episodes.

397   *3.4. Particle I/O ratios*

398   Figure 5 shows the time averaged and size-resolved I/O ratios of particles with diameters of

399   0.01-6.0 µm for two ACMV operation modes (Mode 1: both AC and MV on; Mode 2: AC off

400   and MV on). Table 1 reports the time, date and haze levels of the datasets for the I/O ratios

401   calculation. The small number of entries in Table 1 occurs because we only used datasets

402   when the both indoor and outdoor SMPSs were functioning properly. In both modes, the

403   ACMV system is the major pathway by which outdoor particles migrate indoors.

404   The I/O ratios for all particle sizes are smaller than one, as expected given the absence of any

405   notable indoor particle source. For particles in the size range 0.01-0.2 μm, the mean I/O

406   ratios are in the range of 0.17-0.65 and there is a tendency for the I/O ratio to increase with

407   increasing particle size. For particles of 0.1-1.0 μm, the size-resolved mean I/O ratios are in

408   the range 0.12-0.65. The highest mean I/O ratios occur for particle diameters of

409   approximately 0.3 μm. The mean I/O ratios decrease sharply when the particle size is larger

410   than 0.3 μm. The trend for size-resolved I/O ratios of particles with diameters 0.3-5.0 μm

411   generally agrees with the findings reported by Gupta and Cheong. [32] for ACMV-dominated

412   indoor environments. These findings also align with theoretically predicted results that

413   fibrous particle filters usually have minimum efficiencies for diameters in the range 0.05-0.5

414   μm [11].

415   Figure 5 suggests that, in addition to mechanical ventilation and active filtration, the

416   operation of air conditioning influenced the indoor/outdoor particle ratio. There is a trend

417   such that when the air conditioning was on, the I/O ratios for particles between 0.17 µm and

418   2.5 µm were lower than when the air conditioning was off. Conversely, for particles smaller

419   than about 0.1 µm, there is a tendency for the I/O ratio to be higher when the air conditioning

420   was on as compared to the air-conditioning off state.

421   We have compared the I/O ratios in these two modes using one-way ANOVA tests. The

422   statistical analysis reveals that the differences are statistically significant ($p \leq 0.05$) for

423   particles in all size bins between 0.17 µm and 2.5 µm, except for the size bin 0.3-0.374 µm (p

424   = 0.29). These findings suggest that the ACMV system has higher removal efficiency for

425   particles in this larger size range with active cooling by the air conditioning system.

426   In Singapore's tropical climate, whenever air conditioning is operating, the cooling coil

427   would receive a flow of condensing water from the humid air stream passing over its cooled

428   surfaces. The elevated removal efficiency suggests the possibility of enhanced removal of

429   particles onto the wet surface of the cooling coil when air conditioning is on. The presence of

430   a water film would narrow the gaps between fins. The process of condensation would also

431   induce net transport of particles toward the condensing surfaces through the mechanism of

432   diffusiophoresis. There may also be a thermophoretic influence inducing particle migration

433   from the warmer air toward the cooler fins. It has been recognized that a cooling coil can

434   contribute to removing particles from airstreams [24, 33, 34]. At present, the processes and

435   mechanisms are not well understood and we know of no previously published data of the type

436   presented in Figure 5.

437   For smaller particles, with diameters of 0.01-0.154 µm, we observe a trend of higher I/O

438   ratios when the air conditioning is on compared to when it is off. However, one-way

439 ANOVA results reveal that the differences between the I/O ratios are statistically significant

440 ($p < 0.05$) only for particles in a few size bins, 0.0205–0.0365 µm and 0.0649–0.154 µm.

441 This trend contradicts the theoretically predicted results by Waring and Siegel [34]. In their

442 study, higher deposition rates were predicted for ultrafine particles onto a wet surface than

443 onto the dry surface of a cooling coil. We speculate that the higher I/O ratios that we observe

444 for these smallest particles might be attributable to the growth of ultrafine particles owing to

445 condensation as the air stream is cooled. The condensing species could include water and

446 also semivolatile organic compounds in the air stream whose partitioning between the gas

447 and particle phase is materially influenced by temperature.

448 The information in this study is insufficient to conclusively explain these observations. In

449 future studies, laboratory tests with well-controlled operational parameters could serve to

450 elucidate the influence of cooling coil operation on particle behavior across different size

451 ranges.

452 It is conceivable that variations of outdoor particle concentrations might indirectly influence

453 I/O ratios. However, our data indicate that the difference of time-averaged outdoor particle

454 concentrations between the daytime (AC on) and nighttime (AC off) conditions is relatively

455 small, i.e. less than a 10% difference. Consequently, we consider that variations in outdoor

456 levels did not significantly affect the I/O ratios between the two ACMV operation modes in

457 this investigation.

458   *3.5. Particle removal efficiencies*

459   Figure 6 depicts the time-averaged and size-resolved removal efficiencies of the ACMV

460   system for particles with diameters of 0.01-6.0 μm for two ACMV operation modes (Mode 1:

461   both AC and MV on; Mode 2: AC off and MV on). The single-pass removal efficiencies

462   range from 5% to 80% in both ACMV operation modes, with the respective lowest and

463   highest efficiencies occurring at 0.1 μm and 3.71 μm in Mode 1, and 0.33 μm and 6.0 μm in

464   Mode 2. More specifically, the removal efficiencies are smaller than 30% for particles of

465   diameter 0.01-1.0 μm in Mode 1 and for particles of diameter 0.015-1.12 μm in Mode 2.

466   The size–resolved particle removal efficiencies calculated in the current study have a similar

467   profile with those reported by Azimi et al. [35] (Figure 5 of their paper), which were based on

468   the measured single-pass sized-resolved removal efficiencies for particles of 0.03-10 μm by

469   Hecker and Hofacre. [36].

470   When the mechanical ventilation system was on, indoor air passed through the filters and

471   cooling coil an average of nine times before being replaced by outdoor air, and particle

472   concentrations would diminish during each pass. Consequently, the overall effectiveness of

473   the ACMV system with MERV 7 filters is much higher than the corresponding single-pass

474   efficiency. However, the MERV 7 filters are still insufficient to protect indoor occupants

475   from fine particles of outdoor origin during the haze episode when considering both the low

476   single-pass particle removal efficiencies and the findings reported in Section 3.3. The low

477   removal efficiency of the MERV 7 filters for ultrafine particle also indicates that the filters

478   may fail to protect indoor occupants from ultrafine particles of outdoor origin even during

479   clear-sky periods, when outdoor ultrafine particle number concentrations are elevated

480   (Section 3.2). The high removal efficiencies for particles > 3 μm indicate that the MERV 7

481   filters work effectively to remove the coarse particles. The filters' improved removal

482   efficiencies for coarse particles may be influenced by accumulated particles on the filters as

483   the filters are used.

484   Comparisons of the particle removal efficiencies in the two ACMV operation modes reveal

485   that the removal efficiencies for particles of 0.37- 3.74 μm are significantly higher in the AC

486   on mode than in the AC off mode (one-way ANOVA test, $p < 0.05$). The wet cooling coil

487   surface in the AC on mode results in increases of 4-25% in the removal efficiencies for

488   particles with diameters of 0.37-3.74 μm when compared with the dry cooling coil surface in

489   the AC off mode. The findings suggest that during the haze episode, air conditioning

490   operation could contribute to the attenuation of outdoor particles in this size range in indoor

491   air. However, it is also possible that enhanced particle deposition to wet cooling coil surfaces

492   could contribute to fouling of those surfaces over the long term.

493   **4. Conclusions**

494   During the 2013 haze in Singapore, the outdoor mean size distribution of particles larger than

495   0.2 μm in diameter was remarkably higher than on clear days. Overall, particles of 0.1-1.0

496   μm accounted for large increases, with aggregate volume concentrations that were 5 to 60

497   times higher than during the clear-sky conditions that prevailed a few weeks after the haze

498   episode. There was an evident size shift of the peak particle size to larger diameters within

499   the accumulation mode. This phenomenon might be a consequence of secondary growth of

500   organic aerosol induced by photochemical reactions during the haze.

501   In a mechanically ventilated and air conditioned room on the NTU campus, equipped with

502   MERV 7 grade filters, indoor particles in the size range 0.3-1.0 µm followed the time pattern

503   of outdoor particle concentrations, with some attenuation and a short lag time. The

504   correlations between indoor and outdoor particles in the size range 1.0-2.5 µm were moderate

505   and correlations were not observed for larger particles. Relative to the clear-sky conditions,

506   indoor concentrations of particles in the size range 0.3-2.5 µm increased by factors of 2 to 14

507   during the haze. Any such increase for larger particles was marginal.

508   The mean I/O ratio and removal efficiency of the ACMV system of particles was observed to

509   vary with particle size as would be expected. A conventional ACMV system with MERV 7

510   filters is insufficient to protect building occupants from high exposures to fine particles of

511   outdoor origin under extraordinary circumstances such as the 2013 haze. More effective

512   strategies to protect the public are needed for the recurring transboundary haze.

513   We observed that both I/O ratios and particle removal efficiencies of the ACMV system

514   varied systematically depending on whether or not the air conditioning was on. Information

515   in the current study is insufficient to fully explain these observations. As yet, there is limited

516   scientific knowledge about how pollutants, such particles, semivolatile organic compounds,

517 bioaerosols, and ozone, interact with cooling coil surfaces. More studies that advance our

518 knowledge of these topics are necessary.

526 **References**

527 [1] Amiridis V, Zerefos C, Kazadzis S, Gerasopoulos E, Eleftheratos K, Vrekoussis M, et al.
528   Impact of the 2009 Attica wild fires on the air quality in urban Athens. Atmos Environ
529   2012;46:536-44.
530 [2] Popovicheva O, Kistler M, Kireeva E, Persiantseva N, Timofeev M, Kopeikin V, et al.
531   Physicochemical characterization of smoke aerosol during large-scale wildfires: Extreme
532   event of August 2010 in Moscow. Atmos Environ 2014;96:405-14.
533 [3] Mühle J, Lueker TJ, Su Y, Miller BR, Prather KA, Weiss RF. Trace gas and particulate
534   emissions from the 2003 southern California wildfires. J Geophys Res 2007;112:D03307.
535 [4] Vicente A, Alves C, Calvo AI, Fernandes AP, Nunes T, Monteiro C, et al. Emission
536   factors and detailed chemical composition of smoke particles from the 2010 wildfire
537   season. Atmos Environ 2013;71:295-303.
538 [5] Makkonen U, Hellén H, Anttila P, Ferm M. Size distribution and chemical composition of
539   airborne particles in south-eastern Finland during different seasons and wildfire episodes
540   in 2006. Sci Total Environ 2010;408:644-51.
541 [6] Phoothiwut S, Junyapoon S. Size distribution of atmospheric particulates and particulate-
542   bound polycyclic aromatic hydrocarbons and characteristics of PAHs during haze period
543   in Lampang Province, Northern Thailand. Air Qual Atmos Health 2013;6:397-405.
544 [7] Franzi LM, Bratt JM, Williams KM, Last JA. Why is particulate matter produced by
545   wildfires toxic to lung macrophages? Toxicol Appl Pharm 2011;257:182-8.
546 [8] Huttunen K, Siponen T, Salonen I, Yli-Tuomi T, Aurela M, Dufva H, et al. Low-level
547   exposure to ambient particulate matter is associated with systemic inflammation in
548   ischemic heart disease patients. Environ Res 2012;116:44-51.

549   [9] Wegesser TC, Franzi LM, Mitloehner FM, Eiguren-Fernandez A, Last JA. Lung
550   antioxidant and cytokine responses to coarse and fine particulate matter from the great
551   California wildfires of 2008. Inhal Toxicol 2010;22:561-70.

552   [10] Viswanathan S, Eria L, Diunugala N, Johnson J, McClean C. An analysis of effects of
553   San Diego wildfire on ambient air quality. J Air Waste Manag Assoc 2006;56:56-67.

554   [11] Hinds WC. Aerosol technology: Properties, behavior, and measurement of airborne
555   particles, 2nd edition: John Wiley & Sons, New York.; 1999.

556   [12] Radke LF, Hegg AS, Hobbs PV, Penner JE. Effects of aging on the smoke from a large
557   forest fire. Atmos Res 1995;38:315-32.

558   [13] Niemi JV, Tervahattu H, Vehkamäki H, Martikainen J, Laakso L, Kulmala M, et al.
559   Characterization of aerosol particle episodes in Finland caused by wildfires in Eastern
560   Europe. Atmos Chem Phys 2005;5:2299-310.

561   [14] Klepeis NE, Nelson WC, Ott WR, Robinson JP, Tsang AM, Switzer P, et al. The
562   National Human Activity Pattern Survey (NHAPS): A resource for assessing exposure to
563   environmental pollutants. J Expo Anal Env Epid 2001;11:231-52.

564   [15] Thornburg J, Ensor DS, Rodes CE, Lawless PA, Sparks LE, Mosley RB. Penetration of
565   particles into buildings and associated physical factors. Part I: Model development and
566   computer simulations. Aerosol Sci Tech 2001;34:284-96.

567   [16] Hussein T, Hämeri K, Aalto P, Asmi A, Kakko L, Kulmala M. Particle size
568   characterization and the indoor-to-outdoor relationship of atmospheric aerosols in
569   Helsinki. Scand J Work Environ Health 2004;30 (Suppl 2):54-62.

570   [17] Koponen IK, Asmi A, Keronen P, Puhto K, Kulmala M. Indoor air measurement
571   campaign in Helsinki, Finland 1999 – the effect of outdoor air pollution on indoor air.
572   Atmos Environ 2001;35:1465-77.

573   [18] Matson U. Indoor and outdoor concentrations of ultrafine particles in some Scandinavian
574   rural and urban areas. Sci Total Environ 2005;343:169-76.

575   [19] Wang Y, Hopke PK, Chalupa DC, Utell MJ. Long-term characterization of indoor and
576   outdoor ultrafine particles at a commercial building. Environ Sci Technol 2010;44:5775-
577   80.

578   [20] Morawska L, Jamriska M, Guo H, Jayaratne ER, Cao M, Summerville S. Variation in
579   indoor particle number and PM$_{2.5}$ concentrations in a radio station surrounded by busy
580   roads before and after an upgrade of the HVAC system. Build Environ 2009;44:76-84.

581   [21] Shi B, Ekberg LE, Langer S. Intermediate air filters for general ventilation applications:
582   An experimental evaluation of various filtration efficiency expressions. Aerosol Sci Tech
583   2013;47:488-98.

584   [22] Zhou J, Chen A, Cao Q, Yang B, Chang VWC, Nazaroff WW. Particle exposure during
585   the 2013 Haze in Singapore: Importance of the built environment. Build Environ
586   2015;93:14-23.

587   [23] Azimi P, Stephens B. HVAC filtration for controlling infectious airborne disease
588   transmission in indoor environments: Predicting risk reductions and operational costs.
589   Build Environ 2013;70:150-60.

590 [24] Siegel JA, Nazaroff WW. Predicting particle deposition on HVAC heat exchangers.
591   Atmos Environ 2003;37:5587-96.

592 [25] Wu J, Zhao B. Effect of ventilation duct as a particle filter. Build Environ 2007;42:2523-
593   29.

594 [26] Riley WJ, McKone TE, Lai ACK, Nazaroff WW. Indoor particulate matter of outdoor
595   origin: Importance of size-dependent removal mechanisms. Environ Sci Technol
596   2002;36:200-7.

597 [27] Betha R, Zhang Z, Balasubramanian R. Influence of trans-boundary biomass burning
598   impacted air masses on submicron particle number concentrations and size distributions.
599   Atmos Environ 2014;92:9-18.

600 [28] Mielonen T, Portin H, Komppula M, Leskinen A, Tamminen J, Ialongo I, et al. Biomass
601   burning aerosols observed in Eastern Finland during the Russian wildfires in summer 2010
602   – Part 2: Remote sensing. Atmos Environ 2012;47:279-87.

603 [29] Kulmala M, Vehkamäki H, Petäjä T, Dal Maso M, Lauri A, Kerminen VM, et al.
604   Formation and growth rates of ultrafine atmospheric particles: A review of observations. J
605   Aerosol Sci 2004;35:143-76.

606 [30] Betha R, Spracklen DV, Balasubramanian R. Observations of new aerosol particle
607   formation in a tropical urban atmosphere. Atmos Environ 2013;71:340-51.

608 [31] Nazaroff WW. Indoor particle dynamics. Indoor Air 2004;14 (Suppl 7):175-83.

609 [32] Gupta A, Cheong KWD. Physical characterization of particulate matter and ambient
610   meteorological parameters at different indoor–outdoor locations in Singapore. Build
611   Environ 2007;42:237-45.

612 [33] Jamriska M, Morawska L, Clark BA. Effect of ventilation and filtration on
613   submicrometer particles in an indoor environment. Indoor Air 2000;10:19-26.

614 [34] Waring MS, Siegel JA. Particle loading rates for HVAC filters, heat exchangers, and
615   ducts. Indoor Air 2008;18:209-24.

616 [35] Azimi P, Zhao D, Stephens B. Estimates of HVAC filtration efficiency for fine and
617   ultrafine particles of outdoor origin. Atmos Environ 2014;98:337-46.

618 [36] Hecker R, Hofacre K. Development of performance data for common building air
619   cleaning devices (Final Report No. EPA/600/R-08/013). US Environmental Protection
620   Agency, Office of Research and Development/National Homeland Security Research
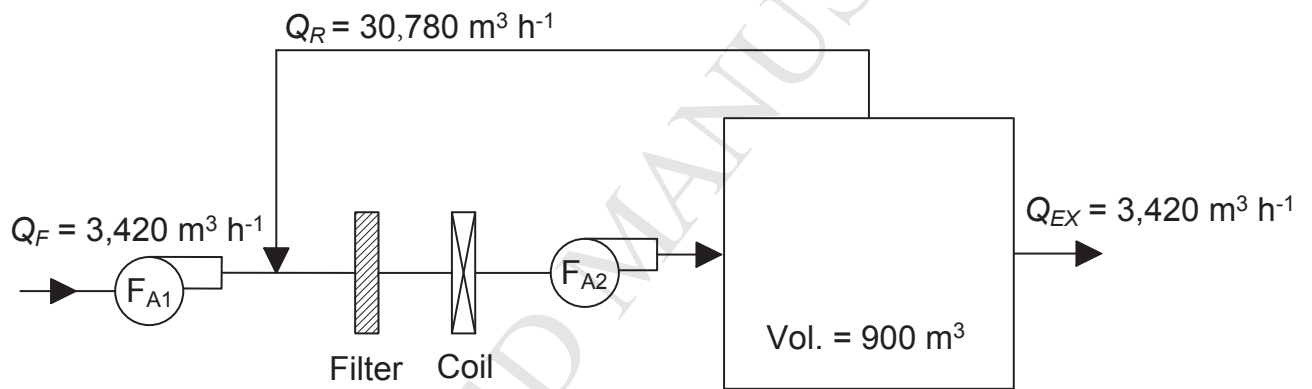621   Center Research Triangle Park, NC 2008.

622

Figure Captions

Figure 1. Schematic representation of the air-conditioning and mechanical ventilation system for the office, illustrating the flow rates (Q), fans (F), filter and coil in the system. For air-flow rates, the subscripts F, R and EX denote forced supply (make-up), recirculation and exfiltration, respectively.

Figure 2. Size-resolved time-averaged outdoor particle volume concentrations ($\mathrm{d}V/\mathrm{d}(\log D_p)$) sorted according to four particle pollution categories. The V value in the legend refers to total average particle volume concentration (0.01-10 µm) in each particle size category.

Figure 3. Size-resolved time-averaged outdoor particle number concentrations ($\mathrm{d}N/\mathrm{d}(\log D_p)$) sorted according to four particle pollution categories. The N value in the legend refers to total average particle number concentration (0.01-10 µm) in each particle size category.

Figure 4. Time-resolved indoor and outdoor particle volume concentrations (dV) in different particle size ranges and for different degrees of haziness.

Figure 5. Size-resolved particle indoor/outdoor (I/O) ratios in two different air-conditioning operation modes (AC on and AC off). Mechanical ventilation was provided at the same volumetric flow rate in both cases. The error bars refer to standard deviations.

Figure 6. Size–resolved particle removal efficiencies (η_i) of the ACMV system in two different air-conditioning operation modes (AC on and AC off). Mechanical ventilation was provided at the same volumetric flow rates in both cases. The error bars refer to standard deviations.

Table 1. Time, date and haze levels used for time-averaged, size-resolved I/O ratio calculations.

AC mode (MV on)	Time	Date	Haziness
AC on	11:21-15:35	14 June 2013	light
	9:00-18:00	17 June 2013	moderate
	13:56-16:59	20 June 2013	heavy
	13:06-17:00	27 June 2013	light
AC off	11:00-14:00	16 June 2013	moderate
	21:00-24:00	22 June 2013	heavy
	21:00-24:00	27 June 2013	light
	00:00-6:00	28 June 2013	light

Q_R = 30,780 m^3 h^{-1}

Q_F = 3,420 m^3 h^{-1}

F_{A1}

Filter   Coil

F_{A2}

Vol. = 900 m^3

Q_{EX} = 3,420 m^3 h^{-1}

Figure 1. Schematic representation of the air-conditioning and mechanical ventilation system for the office, illustrating the flow rates (Q), fans (F), filter and coil in the system. For air-flow rates, subscripts F, R and EX denote forced supply (make-up), recirculation and exfiltration, respectively.
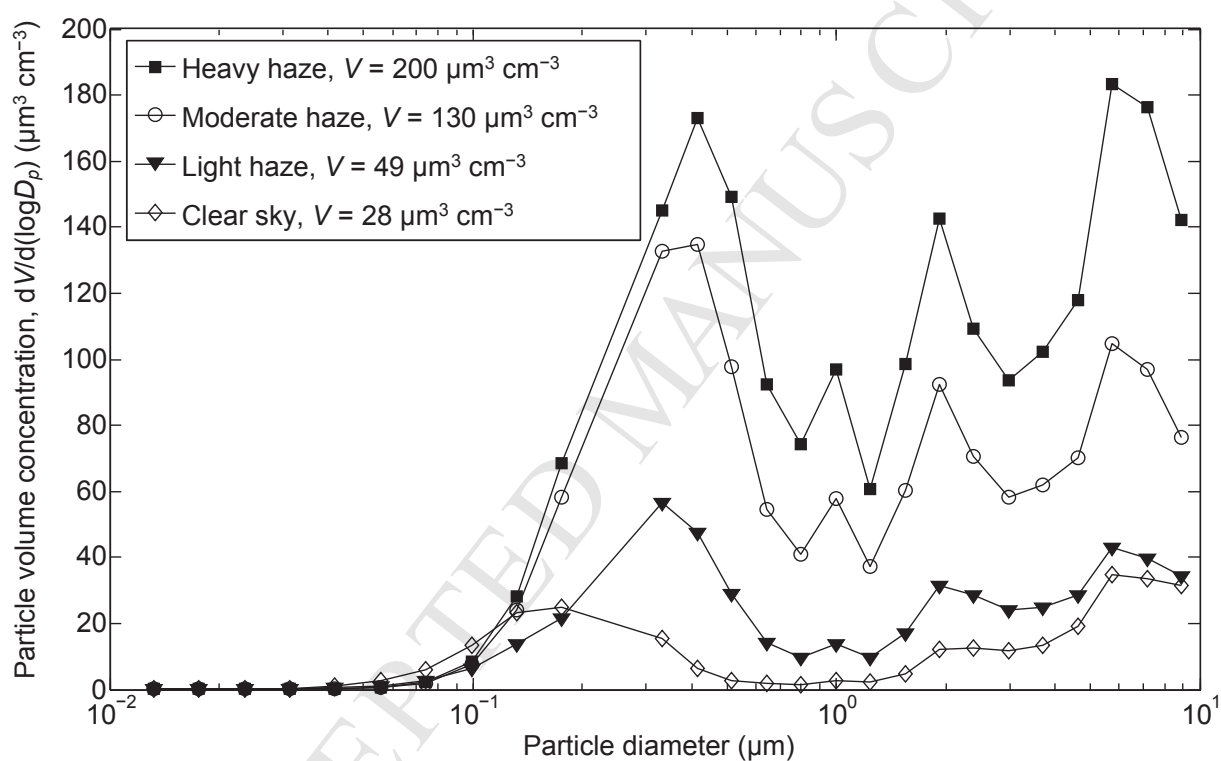
Figure 2. Size−resolved time-averaged outdoor particle volume concentrations ($dV/d(\log D_p)$) sorted according to four particle pollution categories. The V value in the legend refers to total average particle volume concentration (0.01−10 μm) in each particle size category.
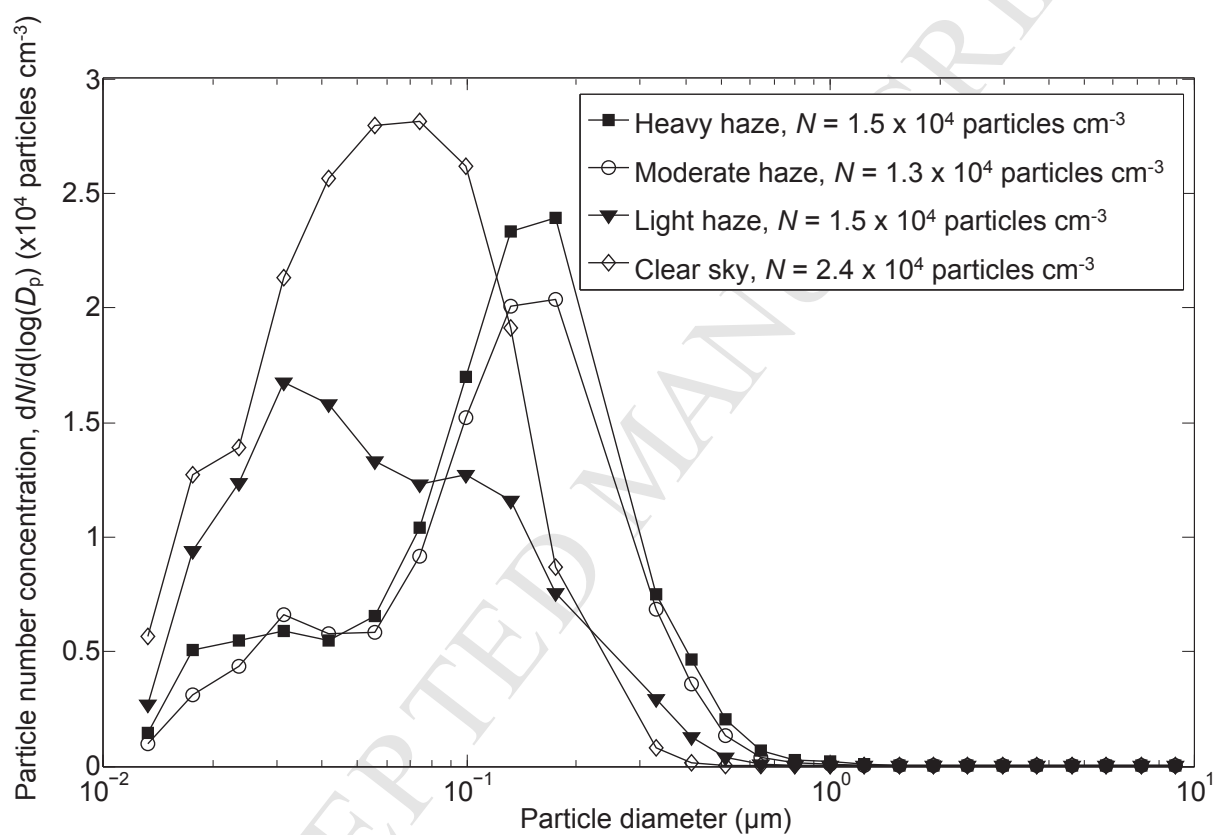
Figure 3. Size−resolved time-averaged outdoor particle number concentrations (dN/d(logD_p)) sorted according to four particle pollution categories. The N value in the legend refers to total average particle number concentration (0.01−10 μm) in each particle size category.
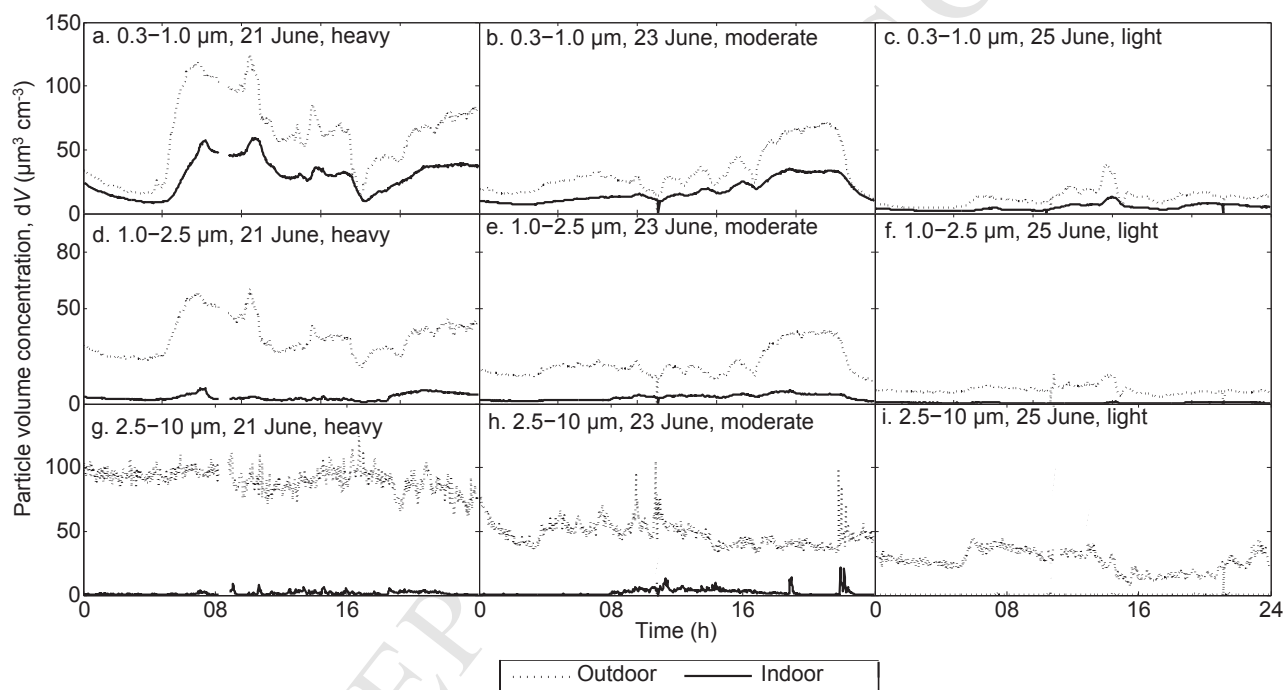
Figure 4. Time-resolved indoor and outdoor particle volume concentrations (dV) in different particle size ranges and for different degree of haziness.
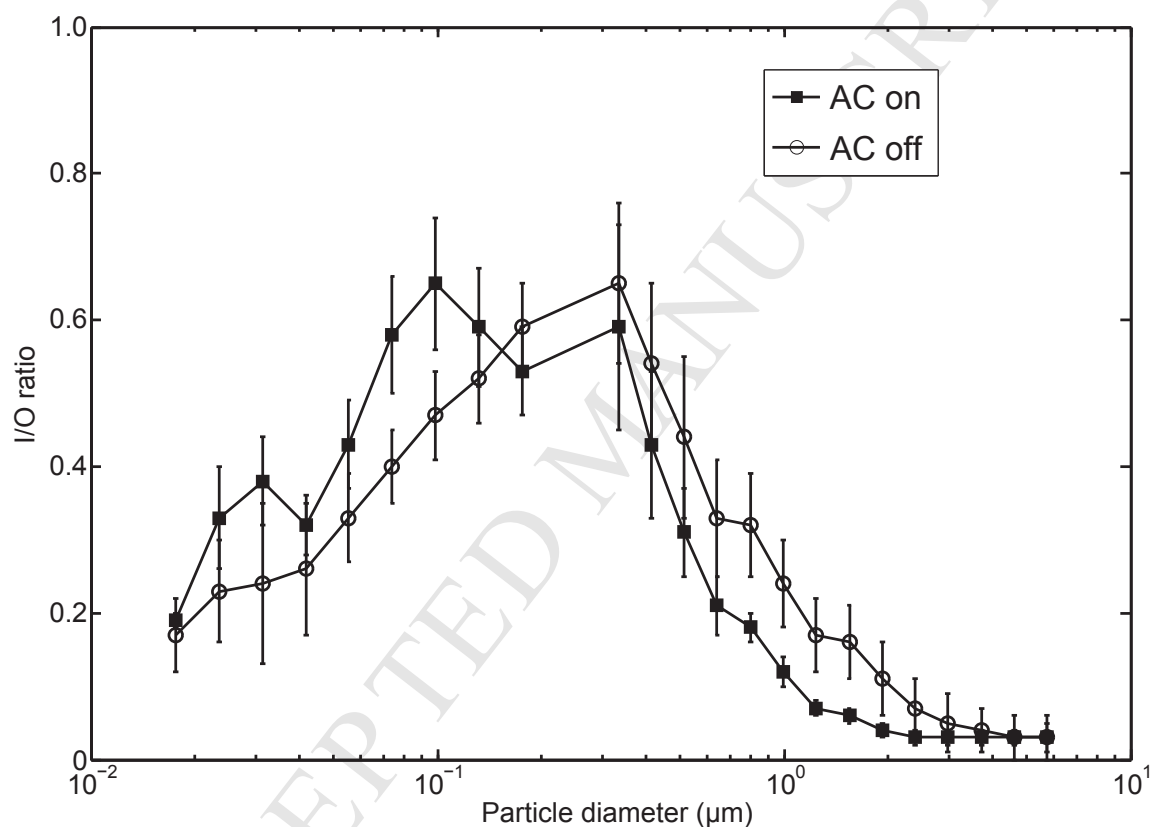
Figure 5. Size-resolved particle indoor/outdoor (I/O) ratios in two different air-conditioning operation modes (AC on and AC off). Mechanical ventilation was provided at the same volumetric flow rates in both cases. The error bars refer to standard deviations.
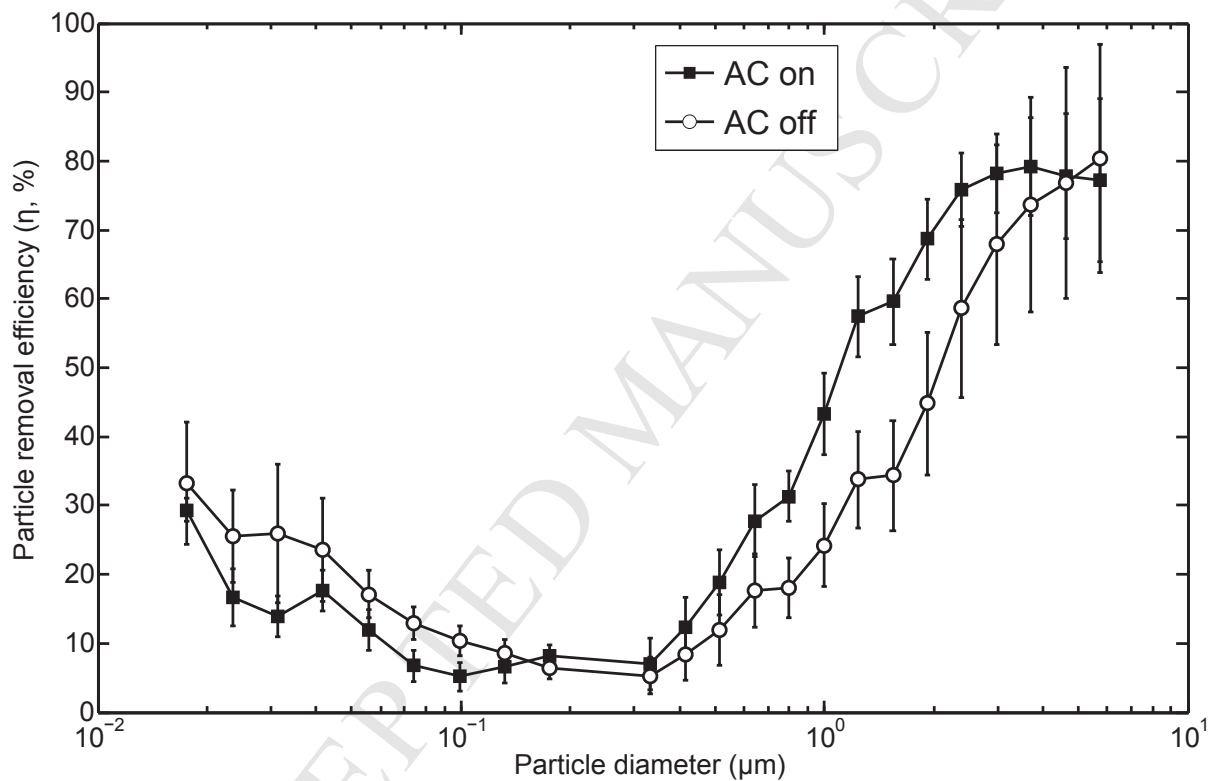
Figure 6. Size−resolved particle removal efficiencies (η_i) of the ACMV system in two different air-conditioning operation modes (AC on and AC off). Mechanical ventilation was provided at the same volumetric flow rates in both cases. The error bars refer to standard deviations.

HIGHLIGHTS (Chen et al., *Building and Environment*, 2015)

- Monitored indoor and outdoor particles during and after the 2013 haze in Singapore.

- Haze mainly causes increases in concentrations of particles larger than ~ 0.2 μm.

- ACMV system attenuated penetration and persistence of outdoor particles indoors.

- AC operation altered the indoor/outdoor concentration ratios of fine particles.

- MERV 7 filters provided < 30% removal efficiencies for particles of 0.01-1.0 μm.